Bioscience, Biotechnology, and Biochemistry

ISSN: (Print) (Online) Journal homepage: https://www.tandfonline.com/loi/tbbb20

# Analysis of the differential expression profile of miRNAs in myocardial tissues of rats with burn injury

Jingdong Guo , Zhensen Zhu , Dongmei Zhang , Bo Chen , Ben Zou , Songying Gao & Xiongxiang Zhu

**To cite this article:** Jingdong Guo , Zhensen Zhu , Dongmei Zhang , Bo Chen , Ben Zou , Songying Gao & Xiongxiang Zhu (2020): Analysis of the differential expression profile of miRNAs in myocardial tissues of rats with burn injury, Bioscience, Biotechnology, and Biochemistry, DOI: 10.1080/09168451.2020.1807901

**To link to this article:** https://doi.org/10.1080/09168451.2020.1807901

BIOSCIENCE, BIOTECHNOLOGY, AND BIOCHEMISTRY
https://doi.org/10.1080/09168451.2020.1807901



# Analysis of the differential expression profile of miRNAs in myocardial tissues of rats with burn injury

Jingdong Guo[a,b], Zhensen Zhu[a,b], Dongmei Zhang[a,b], Bo Chen[a,b], Ben Zou[a,b], Songying Gao[a,b] and Xiongxiang Zhu[a,b]

[a]The Department of Plastic and Burn Surgery, Shenzhen Hospital, Southern Medical University, Shenzhen, China; [b]The Third School of Clinical Medicine, Southern Medical University, Shenzhen, China

**ABSTRACT**

Fifteen percent third-degree burn rat model was used to identify miRNAs that are markers of burn injury-induced myocardial damage. Cardiac tissues were evaluated to determine miRNA profile sequencing. Pearson's correlation analysis was used between miRNAs and injury markers. ROC curve analysis was used to estimate miRNA's sensitivity and specificity for the diagnosis of myocardial damage caused by burn injury. The sequencing analysis revealed 23 differentially expressed miRNAs. Pearson's correlation analysis revealed that rno-miR-190b-3p and C5b9, rno-miR-341, rno-miR-344b-3p and TnI, rno-miR-344b-3p and CK-MB were significantly positively correlated, respectively. ROC curve analysis demonstrated that rno-miR-341, rno-miR-344b-3p, and rno-miR-190b-3p exhibited high sensitivity and specificity for the diagnosis of myocardial damage caused by burn injury. In conclusion, our results suggest that rno-miR-341, rno-miR-344b-3p, and rno-miR-190b-3p have the potential to be used as sensitive and specific biomarkers to diagnose myocardial damage caused by burn injury.

**ARTICLE HISTORY**
Received 12 June 2020
Accepted 2 August 2020

**KEYWORDS**
Myocardial damage; burn injury; miRNA; transcriptome sequencing; biomarker

Approximately 40,000 hospitalizations and nearly 3,000 burn-related deaths caused by burn injuries were reported in the United States in 2014 [1]. Hypermetabolic and hyperinflammatory states caused by burn injuries are characterized by immune dysfunction, muscle protein catabolism, and organ failure [2]. It has been shown that burn injuries induced cardiac dysfunction, including increased cardiac work, systolic dysfunction, tachycardia, and elevated energy expenditure [3]. The human cardiac response to burn trauma is characterized by the ebb and flow phases [3]. After suffering from severe burn trauma, patients experience depression of cardiac contractility, which is referred to as the ebb phase. After 3 days, patients enter the flow phase in which heart rate and cardiac work remain elevated for more than a year [4]. Myocardial cells are damaged in this process, and it will rapidly release substances including CK-MB, LDH, TnI, and so on. Because the content changes of these substances can reflect the degree of myocardial injury and have high myocardial specificity, they are considered as markers of myocardial injury [5,6]. And when myocardial cells necrosis, the C5b9 would be a specific and sensitive marker [7].

MicroRNAs (miRNAs) are a type of endogenous noncoding small RNAs with a length of about 19–23 nucleotides [8]. To regulate the expression of their target genes at the post-transcriptional level, mature miRNAs mainly suppress the translation of their target mRNA by complementary base pairing [9]. miRNAs present in the fluids including urine, serum, plasma, tear and amniotic fluid, and they can resistant to harsh conditions [10]. miRNA also present in exosomes which can be taken up by neighboring or distant cells and subsequently modulate recipient cells [11]. So miRNAs could be a marker of intervention and diagnosis, such as hsa-miR-135a-5p, hsa-miR -542-3, and hsa-miR-4491 maybe the intervention and diagnosis marker of lung cancer via blood test [9]. It has also shown that miRNA can bind to hundreds of target mRNAs and play regulatory roles in almost all mammalian pathological and physiological activities. Furthermore, miRNAs are closely associated with the occurrence and development of several diseases [9]. Some miRNAs related to burn injuries, such as miR-21 which can be affected by heat-induced damage acts in response to the thermal stress by binding to Bcl-2 [12]. miR-29a play an important role in tissue repair and healing of the wound by binding to HEYL and FRS2 to protect the denatured dermis [13]. miR-378a-5p, is involved in wound repair by binding fibroblast growth factor 7 [14]. In addition, some miRNAs, such as miRNA-214 can protect myocardial injury caused by sepsis [15]. let-7i-5p inhibits cardiomyocyte proliferation and repairs heart function post injury by targeting CCND2 and E2F2 [16]. However, miRNAs associated with myocardial injury induced by burn trauma have not yet been identified.

**CONTACT** Xiongxiang Zhu 13991978530@163.com
Supplemental data for this article can be accessed here.

Therefore, we established a rat model of burn injury and used transcriptome sequencing to identify miRNA markers of myocardial injury induced by burn trauma. Then, quantitative real-time polymerase chain reaction (qRT-PCR) was used to investigate differences in the miRNAs expression profile between rats with a burn injury and healthy controls to predict target genes and signaling pathways.

## Materials and methods

### Ethical statement

Animal studies were performed according to standard procedures and experimental protocols and consent procedures were approved by the Animal Ethical and Welfare Committee of Guangzhou Forevergen Medical Laboratory Animal Center (Guangdong, China).

### 15% third-degree burn rat model

Sixteen male SPF rats (6–8 weeks old) with uniform body mass were purchased from Guangdong Experimental Animal Center and fed for 1 week. The 16 rats were randomly divided into a control group and a burn injury group, with 8 rats in each group. The body weight of each rat was weighed, and the burn area was calculated. Before the experiment, SD rats were anesthetized by administering an intraperitoneal injection of 10% chloral hydrate (0.3 mL/100 g). Rats with prone position, the short hairs were removed with 10% sodium sulfide to expose the skin. Several scalded wounds were created on the back of each rat in the burn injury group, and the scalded head was set at a pressure of 0.5 kg at 99°C in 35 s. After scalding, intraperitoneal injection of physiological saline with 30–40 mL/kg was given to prevent shock. The rats were also treated with intramuscular buprenorphine to reduce any associated pain after they recovered from anesthesia. After 24 h, the rats were sacrificed, and myocardial tissues from the whole heart of the rats in each group were obtained and frozen at −80° C, the skin was got and fixed in 4% paraformaldehyde.

### Hematoxylin-eosin (H&E)

The skin was tested according the manual of H&E kit (Beyond, C0105M).

### Enzyme-linked immunosorbent assay (ELISA)

The contents of terminal complement complex (C5b9), creatine kinase-MB (CK-MB), lactate dehydrogenase (LDH), and troponin I (TnI) were determined using an ELISA kit (C5b9: CUSABIO Biotech, CSB-E08709r; CK-MB: Antibodies-online Inc, USA, ABIN955837; LDH: Nanjing Jiancheng Biology Engineering Institute, A020-2; TnI: Abcam, ab174263) according to the manual. Myocardial tissues of the rats were obtained for the detection of burn trauma. 100 mg of myocardial tissue was grinned to powder under liquid nitrogen and then 1 mL phosphate buffer saline was added. The fluid was centrifuged for 20 min, at 4°C, 5000 x *g*. The supernatant was transferred to tube for further test. One hundred microliters of the supernatant and standards of different concentrations were added into microplates and incubated at 37°C for 2 h. The liquid of each well was removed, 100 µL of a biotin-antibody (1X) was added, and then incubated for 1 h at 37°C. The microplates were then washed four times, and 100 µL of horseradish peroxidase-avidin (1X) was added to each well for 1 h at 37°C. The cells were washed five times, and 90 µL of TMB Substrate was added to each well for 30 min. Then, 50 µL of Stop Solution was added to each well to terminate the reaction. Finally, the absorbance was measured using a microplate reader.

### Transcriptome sequencing and analysis of differentially expressed miRNAs

RNA was extracted by the Trizol (Thermo) method according to the manual. Transcriptome sequencing was performed on an Illumina HiSeq2500 platform. The raw data were cleaned by removing the adaptor sequence, reads containing more than 50% bases with a quality value <10, and reads containing >10% unknown bases (N). Clean data were assembled by Trinity software, and differentially expressed miRNAs were obtained using the DESeq R package. MiRNAs with false discovery rate ≤0.001 and showing a 2-fold change were considered as significantly differentially expressed miRNAs.

### GO (gene ontology) and KEGG (Kyoto encyclopedia of genes and genomes) enrichment analysis

The GO knowledgebase is a tool to describe gene and gene product attributes in any organism. The GO project contains three parts: Biological Process (BP), Cellular Component (CC), and Molecular Function (MF). GO analysis was performed to determine the functions of differentially expressed miRNAs. A P-value of <0.05 denoted the significance of GO term enrichment in differentially expressed miRNAs.

KEGG pathway analysis is a functional analysis that involves mapping genes to biological pathways. The pathway with a lower P-value is more significant.

A P-value of <0.05 was used to obtain the high-frequency annotation of the gene set. A GO network map and KEGG enrichment pathway were drawn by the Database for Annotation, Visualization, and Integrated Discovery (DAVID).

### *miRNA–mRNA interaction network analysis*

To explore the interactions among the differentially expressed miRNAs and mRNAs, miRNA–mRNA interaction network analysis was performed using miRWalk2.0 and visualized via Cytoscape.

### *Validation with qRT-PCR*

cDNA synthesis was performed using Reverse Transcriptase (Promega). qRT-PCR was performed using the One-Step SYBR RT-RNA PCR Kit. The expression of U6 was detected as a reference. The relative expression of miRNA was determined by the comparative delta CT ($2^{-\Delta\Delta Ct}$) method. Primer sequences are shown in Supplementary Table 1.

### *Statistical analysis*

All results were analyzed using SPSS 13.0 software. The results were expressed as the mean ± standard deviation of three independent experiments. Pearson's analysis was used to assess associations with myocardial damage factors. A ROC (Receiver Operating Characteristic) curve was generated to assess the relationship between differential miRNAs and myocardial damage caused by burn injury. A Student's t-test was used to compare differences between groups. A p-value of <0.05 was considered as statistically significant.

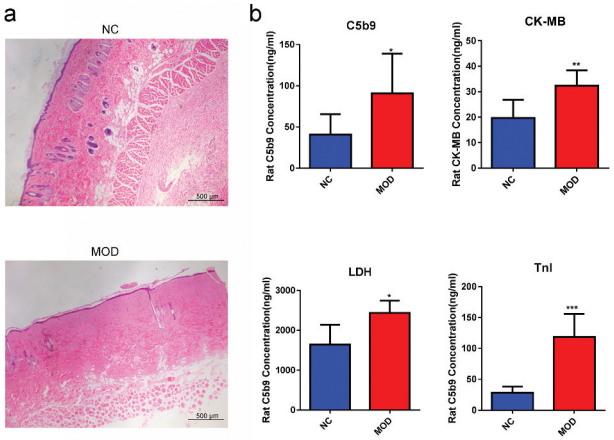


Figure 1. Effects of burn injury on the expression of C5b9, LDH, TnI, and CK-MB in rat myocardial tissues. (a). III burn rat model was validated by H&E staining of skin. (b). The expression levels of C5b9, LDH, TnI, and CK-MB in the burn injury group were significantly upregulated.*p-value < 0.05, **p-value < 0.01.

## Results

### *Detection of myocardial injury markers*

III burn rat model was validated by H&E staining of skin. As shown in Figure 1(a), hair follicles, sweat glands, and nerve endings were damaged in MOD group, which indicated that III burn rat model was constructed successfully. In order to determine whether myocardial injury occurs in the 15% III burn rat model, we detected the myocardial injury associated factors C5b9, CK-MB, LDH, and TnI. It was found that the levels of C5b9, CK-MB, LDH, and TnI were significantly upregulated in the burn injury group compared with the control group (Figure 1(b)). These results indicate that myocardial injury was caused by the burn treatments.

### *Genome-wide analysis of miRNAs and identification of differentially expressed miRNAs*

We took three samples from the control group (NC2, NC6, and NC7) and three from the burn group (MOD1, MOD2, and MOD6), which had relative larger difference between control group and burn group in the content of CK-MB and TnI, for sequencing to determine the miRNA expression profile in myocardial injury caused by burn. Principle component analysis (PCA) (Figure 2(a)) and cluster analysis (Figure 2(b)) demonstrated that MOD6 was highly correlated with the NC group. After removing MOD6, the analysis of differentially expressed miRNAs was performed. It was found that 23 miRNAs were differentially expressed, of which 17 miRNAs were significantly increased, and 6 miRNAs were significantly decreased in the burn injury group (Figure 2(c,d), Table 1).

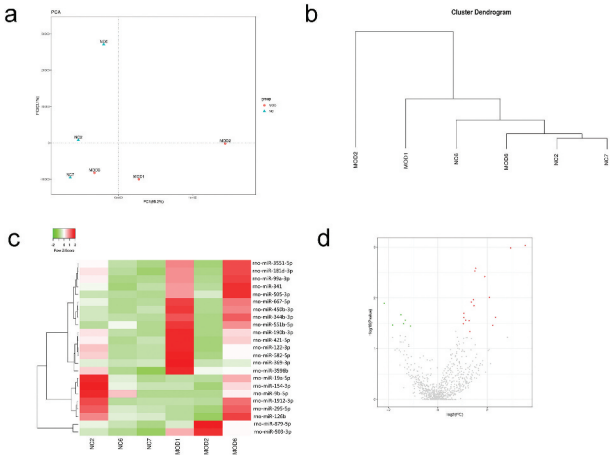


Figure 2. miRNA profiles in myocardial tissues of the normal group and burn injury group. PCA and cluster analyses were used, and the MOD6 sample was removed. Differential expression analysis was then performed. The value of |log2(fold change)| ≥ 1 and p-value < 0.05 were used as standards. A total of 23 differentially expressed miRNA were screened, of which 6 were significantly downregulated, and 17 were significantly upregulated in the burn injury group. (a). PCA analysis. (b). Cluster analysis. c. Heatmap. d. Scatterplot.

Table 1. Differentially expressed miRNAs in the normal group compared with the burn injury group.

| miRNA | NC | MOD | Fold Change | log2(Fold Change) | Up-Down-Regulation | p-value |
|---|---|---|---|---|---|---|
| rno-miR-99a-3p | 4.965 | 13.771 | 2.774 | 1.472 | Up | 0.014 |
| rno-miR-582-5p | 38.067 | 104.427 | 2.743 | 1.456 | Up | 0.011 |
| rno-miR-551b-5p | 5.259 | 10.967 | 2.085 | 1.06 | Up | 0.024 |
| rno-miR-126b | 10.85 | 3.06 | 0.282 | −1.826 | Down | 0.034 |
| rno-miR-344b-3p | 1.84 | 5.358 | 2.912 | 1.542 | Up | 0.003 |
| rno-miR-122-3p | 10.996 | 22.97 | 2.089 | 1.063 | Up | 0.02 |
| rno-miR-421-5p | 5.341 | 11.733 | 2.197 | 1.135 | Up | 0.027 |
| rno-miR-369-3p | 480.761 | 3736.991 | 7.773 | 2.958 | Up | 0.001 |
| rno-miR-181d-3p | 3.774 | 9.695 | 2.569 | 1.361 | Up | 0.012 |
| rno-miR-341 | 18.438 | 45.62 | 2.474 | 1.307 | Up | 0.046 |
| rno-miR-154-3p | 24 | 5.358 | 0.223 | −2.163 | Down | 0.013 |
| rno-miR-503-3p | 34.748 | 176.664 | 5.084 | 2.346 | Up | 0.024 |
| rno-miR-505-3p | 0.92 | 4.332 | 4.709 | 2.235 | Up | 0.035 |
| rno-miR-190b-3p | 17.739 | 50.546 | 2.849 | 1.511 | Up | 0.003 |
| rno-miR-450b-3p | 17.478 | 42.315 | 2.421 | 1.276 | Up | 0.028 |
| rno-miR-295-5p | 43.715 | 16.816 | 0.385 | −1.378 | Down | 0.032 |
| rno-miR-667-5p | 40.943 | 153.602 | 3.752 | 1.908 | Up | 0.004 |
| rno-miR-1912-3p | 13.692 | 6.37 | 0.465 | −1.104 | Down | 0.036 |
| rno-miR-19a-5p | 4.432 | 1.783 | 0.402 | −1.314 | Down | 0.027 |
| rno-miR-3596b | 2.864 | 12.229 | 4.269 | 2.094 | Up | 0.01 |
| rno-miR-3551-5p | 11.018 | 22.704 | 2.061 | 1.043 | Up | 0.032 |
| rno-miR-879-5p | 12.179 | 142.237 | 11.679 | 3.546 | Up | 0.001 |
| rno-miR-9b-5p | 4.286 | 1.527 | 0.356 | −1.489 | Down | 0.021 |

### *Enriched GO terms of differentially expressed miRNAs*

miRNAs usually recognize their target mRNAs by forming a protein–RNA complex through an incomplete complementary base pairing of miRNAs and target mRNAs to block translation of the gene. We used miRNA target gene prediction software to identify miRNA target genes and performed GO and KEGG analysis on these target genes. They were enriched in the BP category, including metabolic process, cellular metabolic process, organic substance metabolic process, primary metabolic process, single-organism, biological regulation, macromolecule metabolic process, cellular macromolecule metabolic process, and the regulation of biological process. They were also enriched in the CC category, including intracellular, cell, cell part, intracellular part, organelle, membrane-bounded organelle, intracellular organelle, intracellular membrane-bounded organelle, cytoplasm, and cytoplasmic part. Lastly, they were enriched in the MF category, including binding, protein binding, heterocyclic compound binding, organic cyclic compound binding, ion binding, metal ion binding, cation binding, catalytic activity, transferase activity, and nucleic acid binding (Figure 3(a)). In general, the target mRNA of differentially expressed miRNAs were major enriched in BP category and CC category, in which metabolic process is the most important.

### *Enrichment analysis of the top 15 KEGG pathways*

Similar to GO analysis, we used miRNA target gene prediction software to predict miRNA target genes and performed KEGG analysis on these target genes. Pathway enrichment analysis based on KEGG was performed through DAVID, and the pathways with $P < 0.05$ were selected. The top 15 KEGG pathways included PI3K-AKT, MAPK, Wnt, and Rap1 signaling pathways (Figure 3(b)). Of note, most of these pathways are related to myocardial injury.

### *miRNA–mRNA interaction analysis*

miRNAs play various kinds of roles by interacting with their target mRNAs. miRNAs with more neighboring proteins are considered more important in BPs. The mRNAs that were enriched in the first 15 KEGG pathways and corresponding miRNAs were

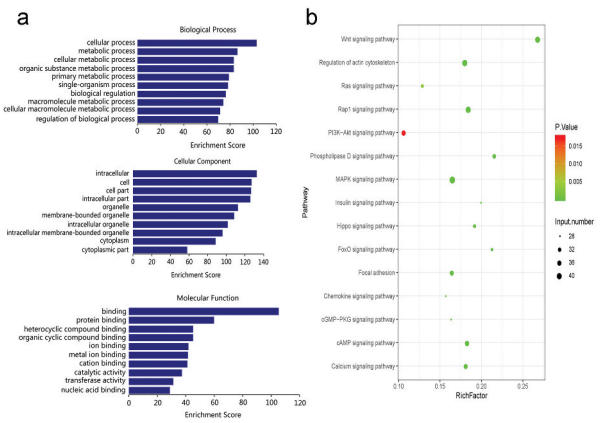


Figure 3. GO and KEGG enrichment analyses of differentially expressed miRNAs in the normal group compared with the burn injury group. Target mRNA of differentially expressed miRNAs were major enriched in BP category and CC category, in which metabolic process is the most important, and miRNA target genes are mainly enriched in PI3K/AKT, MAPK, Wnt, Rap1, and other signal pathways related to myocardial injury. (a). GO enrichment analysis. (b). KEGG enrichment analysis.

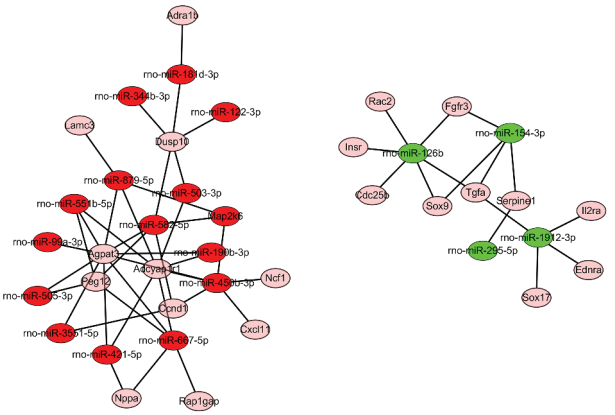


**Figure 4.** miRNA–mRNA interaction network of differentially expressed miRNAs in the normal group compared with the burn injury group. The miRNA–mRNA interaction network was constructed by targeting genes in 15 signaling pathways mapped by KEGG, and only 18 differentially expressed miRNA were selected in the network regulatory map. Red indicated the up-regulated miRNAs green indicated the down-regulated miRNAs, pink indicated the target mRNA.

selected to construct an interaction network. Only 18 miRNAs were found in the regulatory network, which was generated using miRWalk2.0 (Figure 4), the other 5 miRNAs and its target mRNAs were shown in Supplementary Table 2.

### *Validation of candidate miRNAs and correlation analysis*

According to the screening results by transcriptome sequencing, qRT-PCR was performed to verify the differential expression of miRNAs. It was found that rno-miR-667-5p, rno-miR-190b-3p, rno-miR-154-3p, rno-miR-341, rno-miR-99a-3p, rno-miR-344b-3p, rno-miR-122-3p, and rno-miR-879-5p were significantly upregulated in the burn injury group (Figure 5(a)). Of note, the expression level of rno-miR-154-3p in qRT-PCR was opposite to the trend shown by transcriptome sequencing. The results obtained for the other miRNAs were similar to the trends identified by transcriptome sequencing.

Furthermore, Pearson's analysis was used to investigate the relationship between C5b9, TnI, CK-MB, LDH, and miRNAs that showed similar changes to those observed with transcriptome sequencing. The results revealed that rno-miR-190b-3p was significantly positively correlated with C5b9, rno-miR-341 and rno-miR-344b-3p were significantly positively correlated with TnI, and rno-miR-344b-3p was significantly positively correlated with CK-MB, while there are no miRNAs correlated with LDH (Figure 5(b)). Then, ROC curve analysis was used to identify biomarkers, and we found that the area under the curve of rno-miR-341, rno-miR-344b-3p, and rno-miR-190b-3p was 0.891, 0.875, and 0.891, respectively (P-values < 0.05), indicating that these

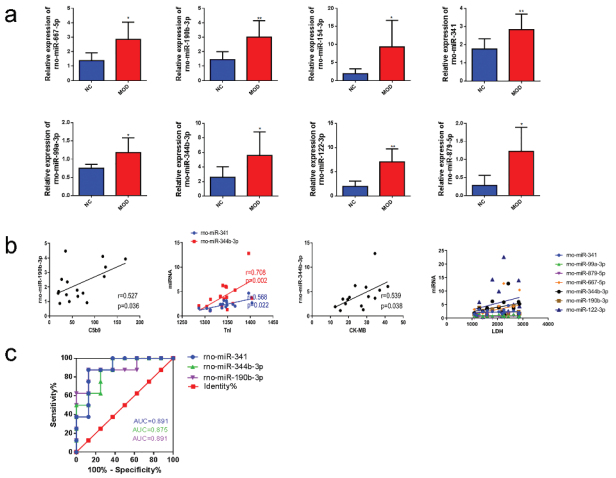


**Figure 5.** Validation of candidate miRNAs and correlation analysis. qRT-PCR of differentially expressed miRNAs in the tissues of normal group compared with the tissue of burn injury group. Pearson's analysis was used to identify the correlation between miRNAs and C5b9, LDH, TnI, and CK-MB. Finally, through ROC curve analysis, the sensitivity of miRNAs related to C5b9, TnI, and CK-MB was evaluated as indicators of burn injury. (a). qRT-PCR identified the differentially expressed miRNAs in the burn injury group compared with the normal group. (b). Pearson's analysis. c. ROC curves.

three miRNAs exhibit high sensitivity and specificity for diagnosing myocardial injury caused by burns (Figure 5(c)).

## Discussion

Severe burn injury often leads to multi-organ dysfunction [3]. It has been reported that progressive cardiac dysfunction after burn trauma occurs, and several animal models of burn injury have been described [3,17]. Animal burn injury models have been used to deepen our understanding of burn injury at the molecular level and identify key factors of post-injury cardiac dysfunction [3]. Several mRNAs involved in burn injury have been found, but the mechanism of burn injury induced by cardiac dysfunction remains unknown. miRNAs are a type of non-coding small RNAs that have been used as biomarkers to diagnose or stage burn injury caused by cardiac dysfunction [18,19]. miR-21, miR-29a, and miR-378a-5p are involved in wound repair, whereas miR-495 inhibits inflammation, differentiation, and extracellular matrix accumulation of cardiac fibroblasts [18–21]. In this study, we identified 23 differentially expressed miRNAs in the burn injury group compared with the normal control group. The differentially expressed miRNAs are mainly involved in PI3K-AKT, MAPK, Wnt, and Rap1 signaling pathways, which are associated with cardiac dysfunction. The PI3K-AKT pathway regulates oxidative stress and cardiac dysfunction in Takotsubo syndrome [22]. Diabetes-induced cardiac dysfunction was associated with attenuation of

the inflammatory response and suppression of the MAPK signaling pathway [23]. Cardiac dysfunction could be induced by transverse aortic constriction through inhibiting the Wnt pathway in mice [24]. Abnormal Rap1 signaling is also associated with cardiac dysfunction [25]. C5b9, LDH, TnI, and CK-MB are important burn injury-induced myocardial infarction markers, and their diagnostic utility in patients with myocardial infarctions has been established [26,27].

miR-190b, which can be detected in tissues and blood in human, is an oncogene that promotes tumorigenesis in several cancers through the regulation of genes, such as Bcl-2, PTEN, and IGF-1 [28–30]. miR-190b promotes cell proliferation, invasion, and migration but decreases cell apoptosis [30]. It has been demonstrated that the expression of miR-190b was dramatically decreased after burn injury [31]. Ectopic expression of miR-190b in myoblast cells inhibited the expression of PHLPP1 and FoxO3a and suppressed cell autophagy by downregulating LC3 and Beclin-1 expression [31]. In our study, the expression of miR-190b was increased in the burn injury group, which may be caused by detection at different degrees of burn injury. miR-190b was also predicted targets Agpat3 and Adcyap1r1 in Figure 4, it is indicated that miR-190b maybe regulate Agpat3 and Adcyap1r1 in the process of cardiac dysfunction, which will need further study. And Pearson's analysis revealed a significant association of miR-190b expression and C5b9. Therefore, miR-190b may provide a new target for diagnosis and therapy. miR-341 belongs to the miR-341~3072 cluster, which encodes 83 miRNAs. It was identified by deep-sequencing that pri-miR-341 is a key target of the TGF-β signaling pathway [32]. The miR-341~3072 cluster is also regulated by Smad2/3-FoxH1 in the early development of embryos [32]. The function of miR-341 has been reported in cancer and neuropathic pain, whereas its role in burn injury is not well understood [33]. In our study, we first demonstrated that miR-341 is upregulated in burn injury-induced cardiac dysfunction. TnI plays an essential role in diastolic function regulation, and its aberrant expression may lead to cardiac diastolic dysfunction, which is a common characteristic of cardiovascular disorders [26]. The levels of miR-341 are closely associated with TnI expression, which indicates the key function of miR-341 in burn injury-induced cardiac dysfunction.

miR-344 was first identified in 2004 in rat cortical neurons [34]. miR-344 contains 19 mature sequences and is expressed during mouse brain development [35,36]. A high throughput microarray study revealed that miR-344 inhibited adipogenesis via the Wnt signaling pathway [37]. In cells, miR-344-inhibited cell differentiation by targeting the Wnt pathway [38]. In addition, miR-344 was implicated in acute respiratory distress syndrome and Huntington's disease [39]. A downstream target of miR-344b is Olig2 [40]. The cardiac expression of miR-344b is affected by sensory neuropathy, but the mechanism is unclear [41]. In our study, we first identified the aberrantly high expression of miR-344b in burn injury-induced cardiac dysfunction. Furthermore, the level of miR-344b was significantly related to the expression of TnI and CK-MB.

In addition, we performed ROC analysis of miR-190b, miR-341, and miR-344b and found that all of these miRNAs were statistically significant. These results indicated that miR-190b, miR-341, and miR-344b exhibit high sensitivity and specificity for diagnosing myocardial dysfunction caused by burn injury.

In conclusion, our study shows that miR-190b, miR-341, and miR-344b are upregulated in the heart tissues of burn injury rats. These miRNAs are significantly associated with myocardial damage biomarkers, which reveal their high sensitivity and specificity for the diagnosis of cardiac dysfunction. Therefore, these results identify potential biomarkers and new drug targets of myocardial dysfunction caused by burn injury.

## Disclosure statement

The authors declare that they have no competing interests.

## Funding

The study was supported by the National Natural Science Foundation of China (grant number No. 81772080).

## Ethics approval

All procedures performed in studies involving animals were in accordance with the ethical standards of the Guangzhou Forevergen Medical Laboratory Animal Center.

## Author contributions

XZ conceived and designed the study, and critically revised the manuscript. JG performed the experiments, analyzed the data and drafted the manuscript. ZZ, DZ, BC, BZ and SG participated in study design, study implementation and manuscript revision. All authors read and approved the final manuscript.

## Availability of data and materials

The datasets generated during and/or analyzed during the current study are available from the corresponding author on reasonable request.

## References

[1] Clayton JL, Edkins R, Cairns BA, et al. Incidence and management of adverse events after the use of laser therapies for the treatment of hypertrophic burn scars. Ann Plast Surg. 2013;70(5):500–505.

[2] Herndon DN, Hart DW, Wolf SE, et al. Reversal of catabolism by beta-blockade after severe burns. N Engl J Med. 2001;345(17):1223–1229.
[3] Guillory AN, Clayton RP, Herndon DN, et al. Cardiovascular dysfunction following burn injury: what we have learned from rat and mouse models. Int J Mol Sci. 2016;17(1):53.
[4] Herndon DN, Tompkins RG. Support of the metabolic response to burn injury. Lancet. 2004;363 (9424):1895–1902.
[5] Jiang SH, Lin CW, Wen F, et al. Role of E-selectin for diagnosis of myocardial injury in children of age up to 14 years. Int J Clin Exp Patho. 2015;8 (9):11206–11211.
[6] Cai W, Yang X, Han S, et al. Notch1 pathway protects against burn-induced myocardial injury by repressing reactive oxygen species production through JAK2/ STAT3 signaling. Oxid Med Cell Longev. 2016;2016:5638943.
[7] Thomsen H, Held H. Susceptibility of C5b-9(m) to postmortem changes. Int J Legal Med. 1994;106 (6):291–293.
[8] Huang D, Wang F, Wu W, et al. MicroRNA-429 inhibits cancer cell proliferation and migration by targeting the AKT1 in melanoma. Cancer Biomark. 2019;26(1):63–68.
[9] He Q, Fang Y, Lu F, et al. Analysis of differential expression profile of miRNA in peripheral blood of patients with lung cancer. J Clin Lab Anal. 2019;33(9): e23003.
[10] Shukla SK, Sharma AK, Bharti R, et al. Can miRNAs serve as potential markers in thermal burn injury: an in silico approach. J Burn Care Res. 2020;41(1):57–64.
[11] Zhang J, Li S, Li L, et al. Exosome and exosomal microRNA: trafficking, sorting, and function. Genom Proteom Bioinf. 2015;13(1):17–24. .
[12] Permenter MG, McDyre BC, Ippolito DL, et al. Alterations in tissue microRNA after heat stress in the conscious rat: potential biomarkers of organ-specific injury. BMC Genomics. 2019;20(1):141.
[13] Zhou J, Zhang X, Liang P, et al. Protective role of microRNA-29a in denatured dermis and skin fibroblast cells after thermal injury. Biol Open. 2016;5 (3):211–219.
[14] Koivisto L, Heino J, Häkkinen L, et al. Integrins in wound healing. Adv Wound Care. 2014;3(12):762–783.
[15] Ge C, Liu J, Dong S. miRNA-214 protects sepsis-induced myocardial injury. Shock. 2018;50(1):112–118.
[16] Hu Y, Jin G, Li B, et al. Suppression of miRNA let-7i-5p promotes cardiomyocyte proliferation and repairs heart function post injury by targetting CCND2 and E2F2. Clin Sci. 2019;133(3):425–441.
[17] White J, Maass DL, Giroir B, et al. Development of an acute burn model in adult mice for studies of cardiac function and cardiomyocyte cellular function. Shock. 2001;16(2):122–129.
[18] Xie J, Zhang L, Fan X, et al. MicroRNA-146a improves sepsis-induced cardiomyopathy by regulating the TLR-4/NF-kappaB signaling pathway. Exp Ther Med. 2019;18(1):779–785.
[19] Wang XW, Jin HY, Jiang SF, et al. MicroRNA-495 inhibits the high glucose-induced inflammation, differentiation and extracellular matrix accumulation of cardiac fibroblasts through downregulation of NOD1. Cell Mol Biol Lett. 2018;23:23.
[20] Sk Sa S, Bharti R. Can miRNAs serve as potential markers in thermal burn injury: an in silico approach. J Burn Care Res. 2020;41(1):57–64.
[21] Zhang D, Chang Y, Han S, et al. The microRNA expression profile in rat lung tissue early after burn injury. Ulus Travma Acil Cerrahi Derg. 2018;24 (3):191–198.
[22] Mao S, Luo X, Li Y, et al. Role of PI3K/AKT/mTOR pathway associated oxidative stress and cardiac dysfunction in takotsubo syndrome. Curr Neurovasc Res. 2020;17(1):35–43.
[23] Gao YL, Kang L, Li CM, et al. Resveratrol ameliorates diabetes-induced cardiac dysfunction through AT1R-ERK/p38 MAPK signaling pathway. Cardiovasc Toxicol. 2016;16(2):130–137.
[24] Pan S, Zhao XJ, Wang X, et al. Sfrpl attenuates TAC-induced cardiac dysfunction by inhibiting Wnt signaling pathway- mediated myocardial apoptosis in mice. Lipids Health Dis. 2018;17(1):202.
[25] Moore SF, Hunter RW, Harper MT, et al. Dysfunction of the PI3 kinase/Rap1/integrin alpha-(IIb)beta 3 pathway underlies ex vivo platelet hypoactivity in essential thrombocythemia. Blood. 2013;121(7):1209–1219.
[26] Pan B, Xu ZW, Xu Y, et al. Diastolic dysfunction and cardiac troponin I decrease in aging hearts. Arch Biochem Biophys. 2016;603:20–28.
[27] Smolenski RT, Forni M, Maccherini M, et al. Reduction of hyperacute rejection and protection of metabolism and function in hearts of human decay accelerating factor (hDAF)-expressing pigs. Cardiovasc Res. 2007;73(1):143–152.
[28] Hung TM, Ho CM, Liu YC, et al. Up-regulation of microRNA-190b plays a role for decreased IGF-1 that induces insulin resistance in human hepatocellular carcinoma. PLoS One. 2014;9(2):e89446.
[29] Wang C, Qiao C. MicroRNA-190b confers radio-sensitivity through negative regulation of Bcl-2 in gastric cancer cells. Biotechnol Lett. 2017;39 (4):485–490.
[30] An NN, Shawn J, Peng JP, et al. Up-regulation of miR-190b promoted growth, invasion, migration and inhibited apoptosis of Wilms' tumor cells by repressing the PTEN expression. Eur Rev Med Pharmaco. 2018;22(4):961–969.
[31] Yu Y, Yang L, Han S, et al. MIR-190B alleviates cell autophagy and burn-induced skeletal muscle wasting via modulating PHLPP1/Akt/FoxO3A signaling pathway. Shock. 2019;52(5):513–521.
[32] Redshaw N, Camps C, Sharma V, et al. TGF-beta /Smad2/3 signaling directly regulates several miRNAs in mouse ES cells and early embryos. Plos One. 2013;8(1):e55186.
[33] Li HX, Shen L, Ma C, et al. Differential expression of miRNAs in the nervous system of a rat model of bilateral sciatic nerve chronic constriction injury. Int J Mol Med. 2013;32(1):219–226.
[34] Kim J, Krichevsky A, Grad Y, et al. Identification of many microRNAs that copurify with polyribosomes in mammalian neurons. Proc Natl Acad Sci U S A. 2004;101(1):360–365.
[35] Liu Q, He HJ, Zeng TB, et al. Neural-specific expression of miR-344-3p during mouse embryonic development. J Mol Histol. 2014;45(4):363–372.
[36] Ling KH, Brautigan PJ, Hahn CN, et al. Deep sequencing analysis of the developing mouse

brain reveals a novel microRNA. Bmc Genomics. 2011;12:176.

[37] Qin LM, Chen YS, Niu YN, et al. A deep investigation into the adipogenesis mechanism: profile of microRNAs regulating adipogenesis by modulating the canonical Wnt/beta-catenin signaling pathway. Bmc Genomics. 2010;11:320.

[38] Chen H, Wang SQ, Chen LX, et al. Micro RNA-344 inhibits 3T3-L1 cell differentiation via targeting GSK3 beta of Wnt/beta-catenin signaling pathway. Febs Lett. 2014;588(3):429–435.

[39] Lee ST, Chu K, Im WS, et al. Altered microRNA regulation in Huntington's disease models. Exp Neurol. 2011;227(1):172–179.

[40] Leong JW, Abdullah S, Ling KH, et al. Spatiotemporal expression and molecular characterization of miR-344b and miR-344c in the developing mouse brain. Neural Plast. 2016;2016:1951250.

[41] Bencsik P, Kiss K, Agg B, et al. Sensory neuropathy affects cardiac miRNA expression network targeting IGF-1, SLC2a-12, EIF-4e, and ULK-2 mRNAs. Int J Mol Sci. 2019;20(4):991.